Polym. Bull. (2012) 69:765–777
DOI 10.1007/s00289-012-0764-4

ORIGINAL PAPER

Facile fabrication of polystyrene/halloysite nanotube microspheres with core–shell structure via Pickering suspension polymerization

Hao Liu · Chaoyang Wang · Shengwen Zou · Zengjiang Wei · Zhen Tong

Received: 15 December 2011 / Revised: 15 April 2012 / Accepted: 2 May 2012 /
Published online: 8 May 2012

Abstract In this article, a facile method for fabrication of core–shell nanocomposite microspheres with polystyrene (PS) as the core and halloysite nanotubes (HNTs) as the shell via Pickering suspension polymerization was introduced. Stable Pickering emulsions of styrene in water were prepared using HNTs without any modification as a particulate emulsifier. The size of the Pickering emulsions varied from 195.7 to 26.7 μm with the water phase volume fraction increasing from 33.3 to 90.9 %. The resulting Pickering emulsions with the water phase volume fraction of above 66.7 % were easily polymerized in situ at 70 °C without stirring. HNTs played an important role during polymerization and effectively acted as building blocks for creating organic–inorganic nanocomposite microspheres after polymerization. The sizes of PS/HNTs microspheres were roughly in accord with that of the corresponding emulsion droplets before polymerization. The effect of the water phase volume fraction on the stability of Pickering emulsions and the morphologies of nanocomposite microspheres was investigated by optical microscopy, confocal laser scanning microscopy, Fourier transform infrared spectroscopy, thermogravimetric analysis, scanning electron microscopy and so on.

Keywords Nanocomposite microspheres · Pickering emulsion · Halloysite nanotube · Suspension polymerization

Introduction

Nowadays, there has been much interest over organic/inorganic core–shell nanocomposites, as they are expected to have combined properties of both the

H. Liu · C. Wang (✉) · S. Zou · Z. Wei · Z. Tong
Research Institute of Materials Science, South China University of Technology, Guangzhou 510640, China
e-mail: zhywang@scut.edu.cn

inorganic nanoparticles and the organic polymers, numerous traditional strategies for improving the interfacial bonding and overall performance of the polymer nanocomposites have been reported [1–4]. Mineral nanoparticles have been extensively studied in the past years as filler materials to improve the interfacial bonding and overall performance of the polymer nanocomposites, combining beneficial properties of both the materials, including low density, flexibility, good modulus, high strength, heat stability, and chemical resistance [5–8].

Halloysite, which is a kind of naturally deposited aluminosilicate, chemically similar to kaolin with an empirical chemical formula of $Al_2Si_2O_5(OH)_4{\cdot}nH_2O$, is a multi-walled inorganic nanotube. The halloysite nanotubes (HNTs) are formed by rolling of a kaolin sheet in preference to tetrahedral rotation to correct the misfit of the octahedral and tetrahedral sheets [9]. Different from most clay, most aluminous components are located in the inner of the HNTs, while in the outer of the HNTs are primarily siloxane and a few silanols and aluminous components which are exposed in the edges of the sheet. HNTs possess numerous hydroxyl groups providing anchoring sites for further modification. Besides, it has high aspect ratio, reasonable mechanical strength, relatively cheap price, and environmental friendly characteristic. Because of these characteristics, it finds a broad range of applications in ceramic material [10], slow release [11], catalyst applications [12], composite materials [13] and so on.

In the past 20 years, colloidal particles or inorganic nanoparticles acted as particulate emulsifiers to stabilize emulsion droplets have attracted an extensive interest since the pioneering work of Pickering [14]. Compared to conventional surfactant systems, not only Pickering emulsions have significant advantages including more stabilization, relatively controlled size, lower toxicity, a reduced rate, and extent of creaming/sedimentation owing to the enhanced viscosity of the continuous phase [15, 16] but also the emulsion droplets can be used as versatile polymerization vessels to fabricate polymer spheres and capsules with supracolloidal structures, which could hold numerous potential for practical applications [17, 18]. Such a surfactant-free emulsion polymerization process, called Pickering emulsion polymerization, is more attractive for preparation of hybrid nanocomposite microspheres than the conventional emulsion polymerization method, owing to no by-products, no unwanted contaminants, and controlled core–shell structure [19].

The research of particulate emulsifiers used to fabricate organic/inorganic core–shell microspheres is mostly focused on a host of synthetic spherical inorganic nanoparticles [20], platelet-like nanoparticles [21], and tube-like nanoparticle [22]. These emulsifiers more or less require synthesis effort or are malignancy to environment, which limit the application in some industrial sectors, for example, agrochemical, biotechnology, catalysis and so on. However, very few attempts have been made to use these platelet- or tube-like mineral nanoparticles to detailedly study Pickering emulsion behavior and further formation of core–shell nanocomposite microspheres via Pickering emulsion template method. Binks et al. [23] prepared an inverse emulsion stabilized by hydrophobically modified bentonite particles. Voorn et al. [24] synthesized polymer/clay nanocomposite latex particles by inverse Pickering emulsion polymerization stabilized with hydrophobic

montmorillonite platelets. Zhang et al. [25] attempted to prepare Pickering emulsion using HNTs grafted with poly(styrene-butylacrylate-acrylic acid) as a particulate emulsifier to stabilize an oil-in-water emulsion.

To the best of our knowledge, non-modified HNTs used as an efficient particulate emulsifier to fabricate core–shell microspheres with HNTs as the shell by Pickering suspension polymerization have not been reported. In this study, we have developed a facile and straightforward Pickering emulsion system based on non-modified HNTs. We explored more details of the factors of Pickering emulsions based on HNTs than Zhang et al. [25] explored. Meanwhile, we first described the preparation of microspheres with polymer cores and HNT shells using a simple approach based on Pickering suspension polymerization that differed from conventional polymerization. Styrene was chosen to be the oil phase of Pickering emulsions. The polymerization factors and the morphology of the fabricated polystyrene (PS) microspheres were analyzed.

Experimental

Materials

HNTs were mined from Yi Chang, Hubei, China. Styrene (Guanghua Chemical Industries Co., China) was distilled under reduced pressure. 2′-Azobisisobutyronitrile (AIBN, Guanghua Chemical Industries Co., China) was recrystallized. Ethanol (Guangzhou chemical Factory, China) was used without further purification. Fluorescein isothiocyanate (FITC) was purchased from Alfa. Hydrofluoric acid (HF, 55 wt%) was purchased from Guangzhou Chemical Reagent Factory. Unless specially stated, all other materials were analytical reagents. Water used in all experiments was purified by deionization and filtration with a Millipore purification apparatus to the resistivity >18.0 MΩ cm.

Purification of HNTs

HNTs were purified according to the Ref. [26]. A typical procedure is described below. A 10 wt% halloysite suspension was prepared by slow addition of water to dry halloysite. Then 0.05 wt% sodium hexametaphosphate was added to the suspension while stirring. The mixture was stirred for 30 min and left to stand for 20 min at room temperature. The clay aggregated. The impurities precipitated in the bottom and were removed by filtration. The filtrate was carefully collected and the resulting HNTs were separated by centrifugation and dried at 80 °C in air for 5 h.

Preparation of Pickering emulsions

In this system, we chose styrene as the oil phase. An aqueous dispersion (0.5 wt%) of HNTs was prepared by adding 0.05 g as-prepared HNTs to 10 mL water with ultrasonication for 3 min. To prepare Pickering emulsions at different water phase volume fractions (Φ_w = 25, 33.3, 36.4, 40, 50, 66.7, 75, 80, 83.3, and 90.9 %),

different volumes of styrene were transferred to the same volume of HNTs aqueous dispersion.

$$\Phi_w = V_w/(V_d + V_w) \times 100\ \% \quad (1)$$

Here, V_w is the water phase volume and V_d is the dispersed phase (oil) volume. The mixtures were homogenized using IKA Ultra Turrax T25 basic instrument at 12,000 rpm for 2 min in an ice bath. The emulsion type was inferred by observing whether a drop of the emulsion dispersed when added to a small volume of water or oil.

Pickering emulsion stabilized by HNTs was labeled with FITC for confocal laser scanning microscopy (CLSM) testing. The fluorescent dye, FITC (5 mg), was dissolved in 5 mL dimethyl sulfoxide (DMSO) at a concentration of 1 mg/mL. The mixture with equal volume (4 mL) of aqueous HNTs dispersion and styrene was homogenized to form Pickering emulsion. 0.8 mL of the dye solution was added to the Pickering emulsion and the mixture system was shaken at 300 rpm for 48 h. Then this Pickering emulsion was washed with water until no free FITC was detected in the water phase.

Preparation of PS/HNT microspheres by Pickering suspension polymerization

Stock styrene containing 1 wt% AIBN was prepared. The as-prepared oil was mixed with an aqueous dispersion of HNTs at different Φ_w, followed by homogenizing at 12,000 rpm for 2 min in an ice bath. The resulting stable Pickering emulsions after nitrogen bubbling through for 15 min were polymerized at 70 °C for 12 h. The produced PS/HNT microspheres were washed three times with ethanol and water, and then dried under vacuum at 40 °C. A part of the microspheres were treated with a certain amount of HF for 48 h to remove the HNTs. The treated microspheres were washed with water to remove the excess HF and dried under vacuum at 40 °C.

A schematic diagram outlining the steps involved in the formation of HNT-based Pickering emulsion and in situ polymerization of styrene in the presence of HNTs is shown in Fig. 1.

Characterization

Zeta-potential of HNTs dispersed in pure water was determined with a Malvern Zetasizer Nano ZS90 and the zeta-potential value was the average of three measurements. The Pickering emulsion droplets were observed with an optical microscope (Carl Zeiss, German) and the number-average diameter was estimated by counting about 200 beads. The prepared emulsions were diluted with their continuous phase for easy observation. The confocal micrographs were taken by a Leica TCS-SP2 CLSM with a 40× objective and a numerical aperture of 1.4. FITC-labeled HNTs were visualized at excitation wavelength of 488 nm. Fourier transform infrared spectra (FTIR) were recorded using a Bruker Vector-33 FTIR spectrometer under ambient conditions. The samples were grounded with KBr and then compressed into pellets. The spectra were taken from 400 to 4,000 cm^{-1}. Thermogravimetric analysis (TGA) was carried out with a NETZSCH TG 209F3

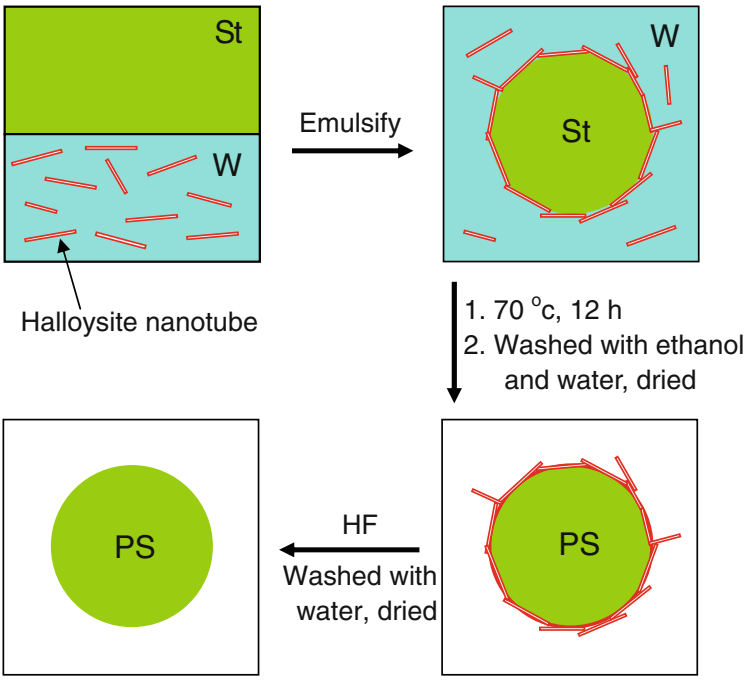

Fig. 1 Schematic illustration of formation of PS/HNTs nanocomposite microspheres by Pickering suspension polymerization

instrument. Samples were heated from 30 to 650 °C at a heating rate of 10 °C/min in nitrogen atmosphere. Gel permeation chromatography (GPC) was carried out by a Waters 717plus Autosampler with 515 HPLC pump, three volumes of styragel HT6, HT4, and HT3, 2414 refractive index detector using tetrahydrofuran (THF, 1 mL/min) as the eluent at 35 °C, and narrowly distributed polystryene (PS) as the standard. Bare PS microspheres after HF treatment were dissolved in THF for 48 h without stirring. The solution was centrifuged and the supernatant was used for measurement. Scanning electron microscopy (SEM) was carried out with a Zeiss EVO 18 electron microscope equipped with a field emission electron gun. The samples were sputter-coated with gold prior to measurement.

Results and discussion

Formation of HNT-based Pickering emulsions

HNTs are naturally occurring silicate nanotubes ubiquitous in soils and weathered rocks. The interlayers of HNTs exist or once existed crystal water, which is the essential characteristic of HNTs different from kaolin. Depending on different mining geographic areas, halloysite deposits have presented in a variety of particle shapes, hydration states, and charge distribution [27]. Figure 2 shows the

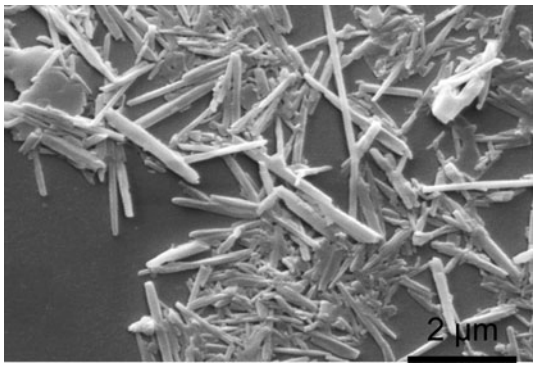

Fig. 2 SEM image of HNTs

morphologies of HNTs formed by dispersion in water and air drying. The lengths of HNTs typically range from 0.5 to 3.0 μm. HNTs after purification steadily scattered in water, and formed a milky suspension.

It is well known that suitable hydrophilicity is crucial for colloidal particles to form stable Pickering emulsions. Hydrophilic particles tend to form oil-in-water (o/w) emulsions whereas hydrophobic particles form water-in-oil (w/o) emulsions [15]. However, Pickering emulsions cannot be formed if particles are highly hydrophilic or highly hydrophobic. The zeta-potential of HNTs is −23.5 mV and suitable for the preparation of o/w Pickering emulsions. In this study, Φ_w (the water phase volume fraction) was chosen to investigate the effect of HNTs on Pickering emulsion, instead of the concentrations of HNTs. As a matter of fact, both the water volume fraction and the concentration of nanoparticles play a similar effect on preparation of Pickering emulsion [28]. Figure 3a shows a series of o/w emulsions prepared at different Φ_w.

We could not obtain emulsions when we attempted to homogenize oil and water phase at $\Phi_w = 25$ %, but we could prepare Pickering emulsions at $\Phi_w = 33.3$ % or above this value, as shown in Fig. 3a. The emulsions prepared at $\Phi_w = 33.3$ % became unstable and a phase separation occurred after standing for 24 h. However, the stable emulsions could be prepared when Φ_w was 36.4 % or higher than this value, these emulsions could keep stable for several weeks. A drop of the emulsions could disperse when added to a small volume of water, which confirmed that the o/w type emulsions were prepared. As water is denser than styrene, residual water appeared below the resulting emulsions, as shown in Fig. 3a. This phenomenon could also confirm the o/w type. According to Binks and coworkers [15], HNTs were supposed to form a close packing structure on the emulsion droplet surfaces if HNTs played a role of a particulate emulsifier. Direct evidence for the adsorption of HNTs on the surface of emulsion droplets is shown in Fig. 3b. HNT-based emulsions were fluorescence labeled with FITC for CLSM testing; FITC could react with hydroxyl groups of HNTs, causing HNTs to show green color by CLSM observation. The fluorescence-labeled HNTs could be observed on the surface of emulsion droplets and displayed a fluorescent ring, suggesting that HNTs indeed closely wrapped up the surface of emulsion droplets.

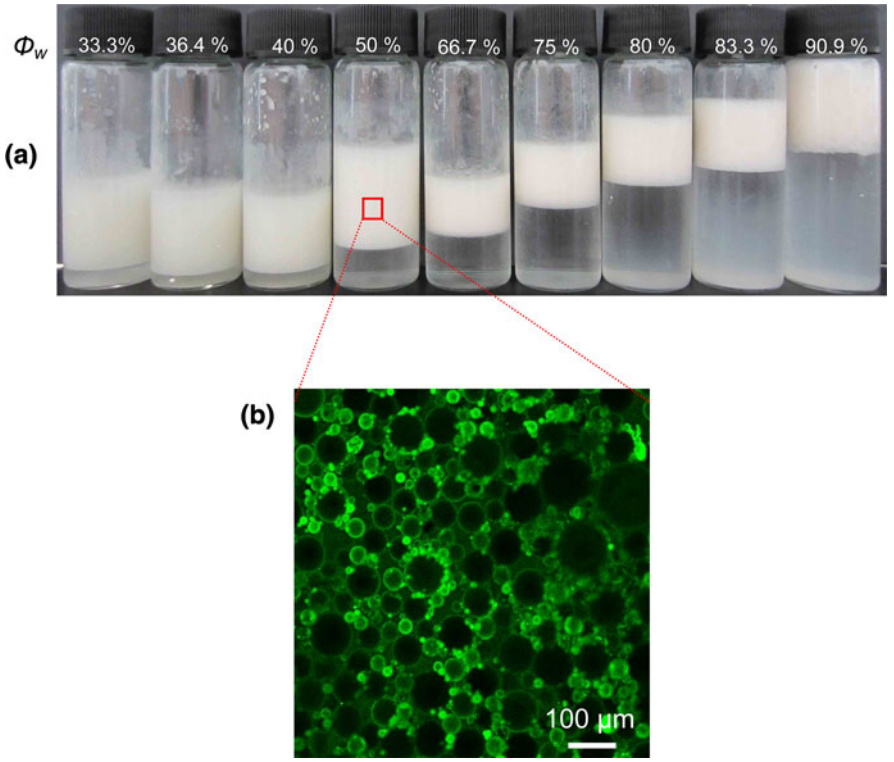

Fig. 3 **a** Digital photographs of HNT-based o/w Pickering emulsions at different Φ_w and **b** confocal image of the emulsion at $\Phi_w = 50$ %

Next, we investigated the morphologies of o/w emulsions preparation at different Φ_w and the results are shown in Fig. 4. It is noted that emulsion droplets were discrete, spherical at various Φ_w. Besides, the sizes of emulsion droplets displayed an obviously change with increasing Φ_w. Figure 5 shows drop size tendency as a function of Φ_w more intuitively. The styrene droplets formed at $\Phi_w = 33.3$ % had a wide-size distribution from several micrometers to nearly 200 μm, which was much larger than the sizes of other emulsions. The ratio of weight of HNTs to volume of oil plays a crucial part in the sizes and the stability of the emulsions. There were so few HNTs at $\Phi_w = 33.3$ % (the small ratio of weight of HNTs to volume of oil) that were not enough to wrap up every small oil droplet. The small oil droplets trended to coalesce to form big oil droplets. So, we could not prepare Pickering emulsions at lower Φ_w (25 % or below this value). At higher Φ_w, enough HNTs made it possible to wrap up every small oil droplet and prevent small oil droplets from coalescence. Thus, small droplets were obtained and the emulsions showed a good stability. With increasing Φ_w (also the ratio of weight of HNTs to volume of oil), the droplet size decreased first and then became nearly constant when excess HNTs in the continuous phase appeared in Fig. 3a.

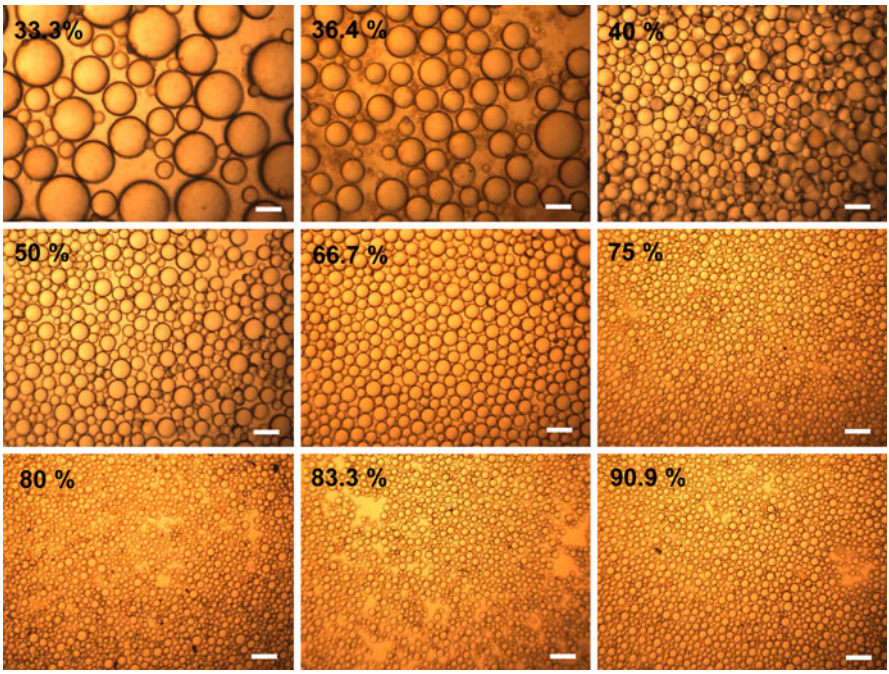

Fig. 4 Optical micrographs of HNTs-based o/w Pickering emulsions. *Scale bars* 50 μm

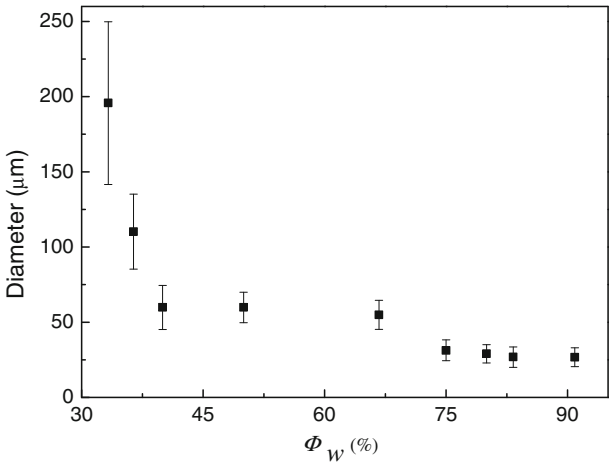

Fig. 5 Mean droplet diameter of emulsion droplets as a function of Φ_w. *Error bars* Standard deviation ($n = 200$)

Preparation and characterization of PS/HNT nanocomposite microspheres

Pickering emulsions preparation at low Φ_w tended to break up when it was applied to the polymerization process. So, we chose four typical Φ_w (66.7, 75, 83.3, and

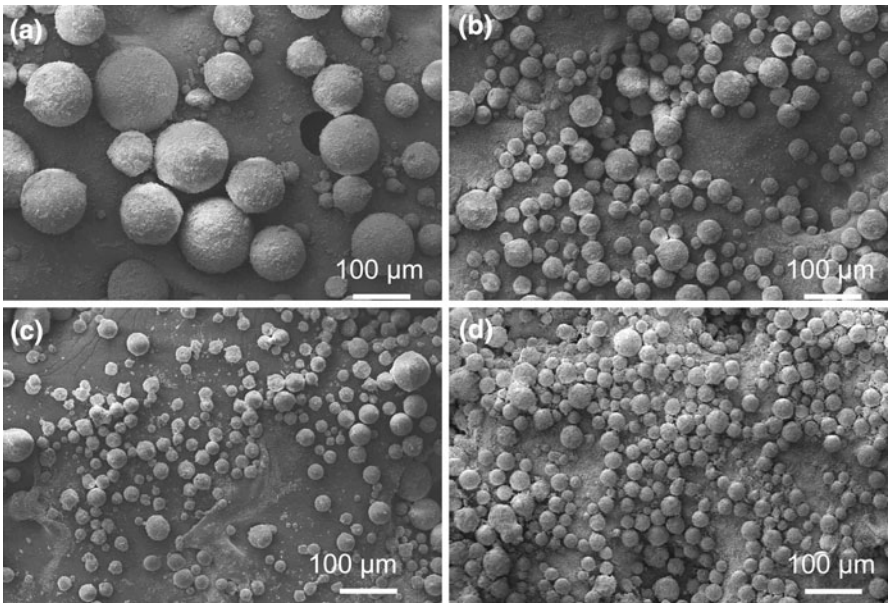

Fig. 6 SEM images of PS/HNT nanocomposite microspheres preparation at different Φ_w, **a** 66.7 %, **b** 75 %, **c** 83.3 %, and **d** 90.9 %

90.9 %) to analyze the polymerization condition. Polymerization could be easily carried out and needed no stirring after generation of a robust Pickering emulsion. Figure 6a–d shows the surface morphologies of the as-prepared PS/HNT microspheres at different Φ_w. These photographs displayed a decreasing tendency in microsphere size with increasing Φ_w. Besides, hybrid PS microspheres still kept spherical, and the surface was rough. The sizes of PS microspheres roughly accorded with that of the corresponding emulsion droplets before polymerization and had a size distribution as wide as that of the original Pickering emulsions, indicating that the high stabilization of the HNT-based Pickering emulsions for successful suspension polymerization to produce the microspheres with controlled morphology.

Figure 7a, b shows SEM images of the same sample as described in Fig. 6b but at a higher magnification. We could clearly see the tube-like HNTs on the surface of PS microspheres in Fig. 7a, b. It was surprising to find that there were some small PS nanospheres on the surface of big PS microsphere. This phenomenon was most likely that styrene and AIBN had certain solubility in water, which resulted in a low degree of polymerization of styrene on the surface of big PS microspheres. After HF treatment (Fig. 7c, d), the surface of PS microspheres was clean and smooth, and no HNTs were observed on the surface of PS microspheres. EDS analyses further showed that HNTs were embedded into the surface of PS microsphere before HF treatment, and HNTs were removed from the surface after HF treatment. The number-average molecular weight (M_n) of PS in the nanocomposites after HF treatment is 3.6×10^4, 5.1×10^4, 4.3×10^4, and 4.7×10^4 with similar PDI

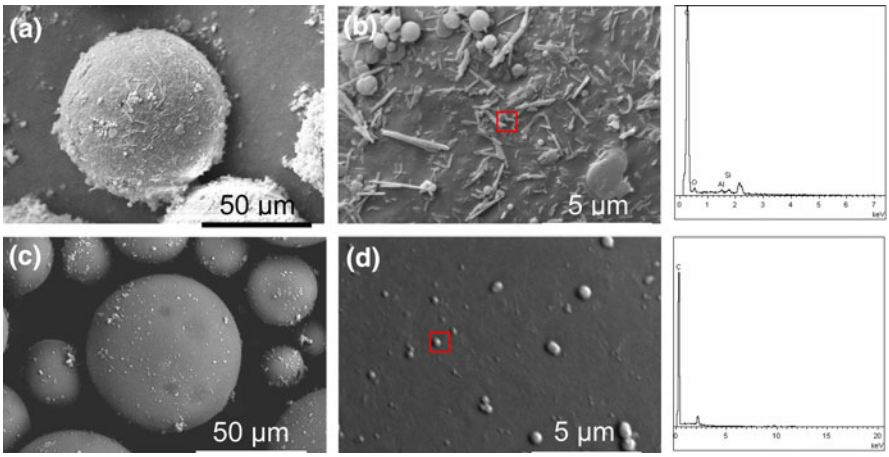

Fig. 7 SEM images of PS/HNT nanocomposite microspheres preparation at $\Phi_w = 75$ % at low (**a**, **c**) and high (**b**, **d**) magnification with EDS analysis, before (**a**, **b**) and after (**c**, **d**) washing with HF

values from 3.2 to 4.0 for four batches of $\Phi_w = 66.7$, 75, 83.3, and 90.9 %, respectively. Φ_w has an unobvious effect on M_n which is typical for suspension polymerization of styrene.

The above SEM images and EDS analysis confirmed that each colloidal particle of PS had HNTs adsorbed on the surface, and PS microspheres themselves did not aggregate to form large agglomerates. Obviously, HNTs acted as an effective stabilizer during polymerization and as building blocks for creating the organic–inorganic nanocomposite microspheres after polymerization.

Figure 8 shows the FTIR spectra of the HNTs, the PS/HNT nanocomposites, and the bare PS produced. The absorption bands at 3,696 and 3,621 cm^{-1} in Fig. 8a could be attributed to stretching vibrations υ (–OH) of HNTs (Kaolin has four absorption bands in this high frequency area, 3700, 3670, 3650, 3200 cm^{-1}), and those bands at 1031, 910 cm^{-1} were attributed to stretching vibrations (Si–O–Si) and flexural vibrations (Al–O–H). The flexural vibrations peak of Si–O at 469 cm^{-1} for HNTs was observed in the FTIR spectra of the HNTs and PS/HNT nanocomposites. The characteristic peaks of PS, such as flexural vibrations (C–H) of the benzene ring at 698 and 755 cm^{-1}, stretching vibrations (C–C) of benzene ring at 1448, 1491, and 1600 cm^{-1}, the flexural vibrations of the benzene ring at 3025, 3059, 3081 cm^{-1} and overtones of mono-sub benzene at 1760–1900 cm^{-1}, were present in the FTIR spectra of the bare PS and PS/HNT nanocomposites. The presence of peaks at bands 1, 2, 3, along the appearance of weak peak at 469 cm^{-1} in Fig. 8b indicated that we had successfully fabricated composite PS/HNT microspheres. Compared with Fig. 8b, the absorption band at 469 cm^{-1} disappeared in Fig. 8c, suggesting that we had obtained bare PS microspheres after HF treatment.

Figure 9 presents the thermal degradation behaviors of the composite microspheres prepared at different Φ_w. TGA is used to determine the total inorganic content in the composite microspheres. All PS/HNT composite microspheres follow similar decomposition tendency with exhibiting two-stage decompositions. The first

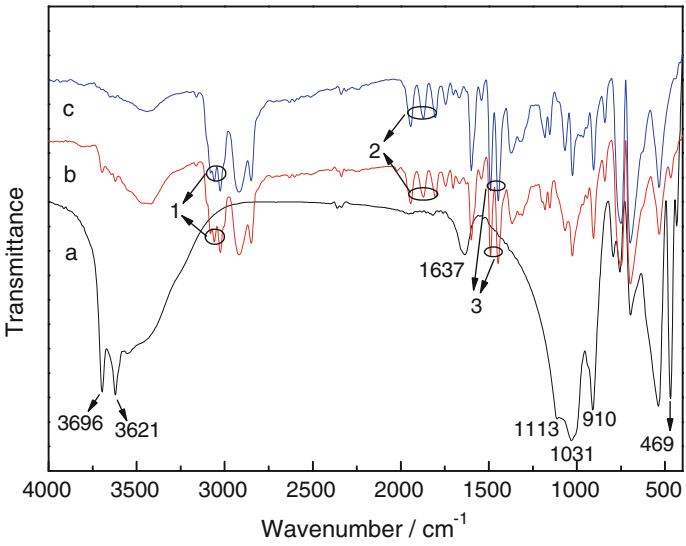

Fig. 8 FTIR of (*a*) HNTs, (*b*) PS/HNT nanocomposite microspheres, and (*c*) PS microspheres

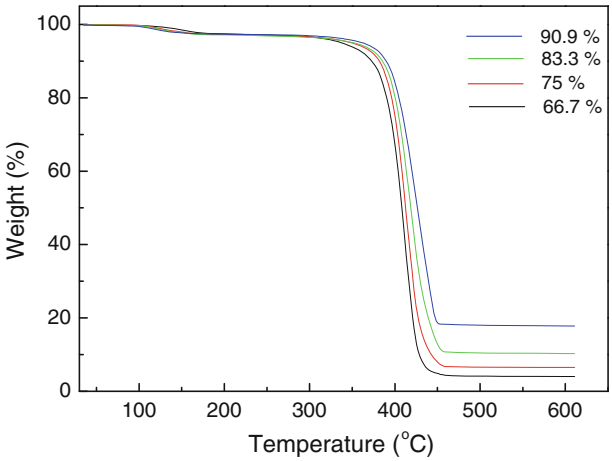

Fig. 9 TGA curves of PS/HNT nanocomposite microspheres

stage was in the temperature region of 100–170 °C, which was probably related to the evaporation of adsorption water in interlayers of HNTs. The second one started at about 300 °C. The maximum decomposition rate of the products was found at around 400 °C, attributed to the decomposition of PS. The residues above 450 °C were mainly the HNTs left behind. There were about 95.9, 93.5, 89.5, and 82.2 wt% weight loss at 500 °C for $\Phi_w = 66.7$, 75, 83.3, and 90.9 %, respectively. According to Fig. 6, PS/HNT microspheres became smaller with increasing Φ_w, which leaded to an increase of a relative content of HNTs in microspheres, following an increase of residual HNTs after decomposition. The decomposition tendency was in well agreement with the effect of Φ_w on polymerization.

Conclusion

In summary, nanocomposite microspheres consisting PS cores and HNTs shells were prepared by Pickering suspension polymerization of styrene as oil was based on HNTs. We mainly focused on the effects of the water phase volume fraction to the sizes and morphologies of styrene in water Pickering emulsions and the produced nanocomposite microspheres. We had demonstrated that the mean size of emulsion droplets and PS microspheres decreased along with the increase of Φ_w until a limiting size was reached when excess HNTs in the continuous phase appeared. So, we could control the size of emulsion droplets and PS microspheres in the range of a few tens of micrometers by varying Φ_w. CLSM observation showed that HNTs indeed closely wrapped up the surface of emulsion droplets, and the coarse surface of the microspheres from SEM clearly suggested that the hydrophilic HNTs were located at the microsphere surface.

The above results showed that Pickering emulsion droplets could be used as polymerization vessels to fabricate core–shell nanocomposite microspheres. The emulsions based on HNTs had a high stabilization during the suspension polymerization process. This polymerization method offers a facile route to fabricate a variety of hybrid microspheres with supracolloidal structures. Besides, these core–shell microspheres have the potential to be used as synergistic reinforcement fillers in fabricating high-performance and functional nanocomposites.

Acknowledgments This study was supported by the National Basic Research Program of China (973 Program, 2012CB821500), the National Natural Science Foundation of China (50973034), and the Fundamental Research Funds for the Central Universities.

References

1. Chen B, Deng JP, Tong LY, Yang WT (2010) Optically active helical polyacetylene@silica hybrid organic-inorganic core/shell nanoparticles: preparation and application for enantioselective crystallization. Macromolecules 43:9613–9619
2. Cha′vez JL, Wong JL, Duran RS (2008) Core-shell nanoparticles: characterization and study of their use for the encapsulation of hydrophobic fluorescent dyes. Langmuir 23:2064–2071
3. Armini S, Vakarelski IU, Whelan CM, Maex K, Higashitani K (2007) Nanoscale indentation of polymer and composite polymer-silica core–shell submicrometer particles by atomic force microscopy. Langmuir 23:2007–2014
4. Niu ZW, Yang ZZ, Hu ZB, Lu YF, Han CC (2003) Polyaniline-silica composite conductive capsules and hollow spheres. Adv Funct Mater 13:949–954
5. Mohsen-Nia M, Mohammad Doulabi FS (2011) Synthesis and characterization of polyvinyl acetate/montmorillonite nanocomposite by in situ emulsion polymerization technique. Polym Bull 66:1255–1265
6. Alexandre M, Dubois P (2000) Polymer-layered silicate nanocomposites: preparation, properties and uses of a new class of materials. Mater Sci Eng 28:1–63
7. Usuki A, Hasegawa N, Kato M (2005) Polymer–clay nanocomposites. Adv Polym Sci 179:135–195
8. Bao Y, Ma JZ (2011) Polymethacrylic acid/Na–montmorillonite/SiO_2 nanoparticle composites structures and thermal properties. Polym Bull 66:541–549
9. Singh B (1996) Why does halloysite roll?—A new model. Clays Clay Miner 44:191–196
10. Wilson IR (2004) Kaolin and halloysite deposits of China. Clay Miner 39:1–15
11. Kelly HM, Deasy PB, Ziaka E, Claffey N (2004) Formulation and preliminary in vivo dog studies of a novel drug delivery system for the treatment of periodontitis. Int J Pharm 274:167–183

12. Cho KH, Jang BS, Kim KH (2006) Performance of pyrophyllite and halloysite clays in the catalytic degradation of polystyrene. React Kinet Catal Lett 88:43–50
13. Liu MX, Guo BC, Zou QL, Du ML, Jia DM (2008) Interactions between halloysite nanotubes and 2,5-bis(2-benzoxazolyl) thiophene and their effects on reinforcement of polypropylene/halloysite nanocomposites. Nanotechnology 19:205709–205809
14. Pickering SU (1907) Emulsions. J Chem Soc Trans 91:2001–2021
15. Aveyard R, Binks BP, Clint JH (2003) Emulsions stabilised solely by colloidal particles. Adv Colloid Interface Sci 503:100–102
16. Niu Z, He J, Russell TP, Wang Q (2010) Synthese von nano-/mikrostrukturen an fluiden grenzflächen. Angew Chem 122:10250–10265
17. Wang CY, Liu HX, Gao QX, Liu XX, Tong Z (2007) Facile fabrication of hybrid colloidosomes with alginate gel cores and shells of porous $CaCO_3$ microparticles. Chem Phys Chem 8:1157–1160
18. Zhao YL, Wang HT, Song XM, Du QG (2010) Fabrication of two kinds of polymer microspheres stabilized by modified titania during Pickering emulsion polymerization. Macromol Chem Phys 211:2517–2529
19. Hasell T, Yang JX, Wang WX, Li J, Brown PD, Poliakoff M, Lester E, Howdle SM (2007) Preparation of polymer–nanoparticle composite beads by a nanoparticle-stabilised suspension polymerisation. J Mater Chem 17:4382–4386
20. Song XM, Zhao YL, Wang HT, Du QG (2009) Fabrication of polymer microspheres using titania as a photocatalyst and Pickering stabilizer. Langmuir 25:4443–4449
21. Cauvin S, Colver PJ, Bon SAF (2005) Pickering stabilized miniemulsion polymerization: preparation of clay armored latexes. Macromolecules 38:7887–7889
22. Zhang C, Liu TX, Lu XH (2010) Facile fabrication of polystyrene/carbon nanotube composite nanospheres with core–shell structure via self-assembly. Polymer 51:3715–3721
23. Binks BP, Clint JH, Whitby CP (2005) Rheological behavior of water-in-oil emulsions stabilized by hydrophobic bentonite particles. Langmuir 21:5307–5316
24. Voorn DJ, Ming W, Van Herk AM (2006) Polymer clay nanocomposite latex particles by inverse Pickering emulsion polymerization stabilized with hydrophobic montmorillonite platelets. Macromolecules 39:2137–2143
25. Zhang YW, Jiang JQ, Liang QH, Zhang B (2009) Modification of halloysite nanotubes with poly(styrene-butyl acrylate-acrylic acid) via in situ soap-free graft polymerization. J Appl Polym Sci 117:3054–3059
26. Shchukin DG, Sukhorukov GB, Price RR, Lvov YM (2005) Halloysite nanotubes as biomimetic nanoreactors. Small 1:510–513
27. Qian D, Dickey EC, Andrews R, Rantell T (2000) Load transfer and deformation mechanisms in carbon nanotube-polystyrene composites. Appl Phys Lett 76:2868–2871
28. Binks BP, Lumsdon SO (2001) Pickering emulsions stabilized by monodisperse latex particles: effects of particle size. Langmuir 17:4540–4547